HHS Public Access

Author manuscript

Nature. Author manuscript; available in PMC 2018 October 25.

Published in final edited form as:

Nature. 2018 April ; 556(7702): 447–451. doi:10.1038/s41586-018-0042-1.

Quaternary Stereocenters via an Enantioconvergent Catalytic S_N1 Reaction

Alison E. Wendlandt, **Prithvi Vangal**, and **Eric N. Jacobsen***

Department of Chemistry and Chemical Biology, Harvard University, 12 Oxford St, Cambridge MA 02138

Abstract

The unimolecular nucleophilic substitution (S_N1) mechanism figures prominently in every introductory organic chemistry course. In principle, stepwise displacement of a leaving group by a nucleophile via a carbocationic intermediate allows for the construction of highly congested carbon centers. However, the intrinsic instability and high reactivity of the carbocationic intermediates render it very difficult to control product distributions and stereoselectivity in reactions proceeding via S_N1 pathways. Here we report asymmetric catalysis of an S_N1-type reaction mechanism resulting in the enantioselective construction of quaternary stereocenters from racemic precursors. The new transformation relies on the synergistic action of a chiral hydrogen bond donor (HBD) catalyst with a strong Lewis acid promoter to mediate the formation of tertiary carbocationic intermediates at low temperature and achieve high levels of control over reaction enantioselectivity and product distribution. The work presented here provides a foundation for the enantioconvergent synthesis of other fully-substituted carbon stereocenters.

Quaternary stereogenic centers are important structural motifs in natural products and biologically-active compounds, conferring valuable structural, conformational and metabolic properties. Their construction has long been recognized as an important challenge to the field of chemical synthesis, and several distinct catalytic, enantioselective approaches have been developed in response.[1,2,3,4] Notable examples include cycloadditions,[5] α and β-alkylation and arylation of carbonyls,[6–8] 3,3′-additions,[9] S_N2' reactions,[10] and Heck-type cross-couplings.[11] Each of these very powerful methods relies on enantiofacial addition across a *prochiral substrate* (Figure 1a) and therefore requires the preparation of stereochemically well-defined starting materials (such as trisubstituted olefins), and subsequent enantioselective bond formation.

* jacobsen@chemistry.harvard.edu.

Correspondence and requests for materials should be addressed to E.N.J. (jacobsen@chemistry.harvard.edu).

Author Contributions A.E.W. and E.N.J. conceived the work, A.E.W. and P.V. conducted the experiments, E.N.J. directed the research, and A.E.W, P.V. and E.N.J wrote the manuscript.

The authors declare no competing financial interests.

Data Availability CCDC 1822228 contains the crystallographic data for compound **5b**•HCl. These data can be obtained free of charge from the Cambridge Crystallographic Data Center (www.ccdc.cam.ac.uk). Raw data for kinetics experiments are available on request. The authors declare that all other data supporting these findings are available within the paper or the Supplementary Information.

We envisioned that stepwise nucleophilic substitution reactions proceeding through prochiral carbocationic intermediates could provide a useful and complementary strategy for the enantioselective synthesis of compounds bearing quaternary stereocenters. Unlike the synthetic approaches noted above, quaternary-stereocenter construction via an S_N1-like pathway might be stereoablative[12] and thus could engage readily accessed racemic compounds as substrates (Figure 1b). While realization of this strategy would lift the requirement for stereocontrol in the synthesis of the substrate, it would also require overcoming several very significant challenges. The requisite catalytic system must (a) generate a reactive tertiary carbocationic intermediate, (b) minimize undesired elimination and rearrangement pathways, and (c) exert enantiocontrol in additions of a *C*-centered nucleophile to a high energy cationic intermediate. Indeed, despite the practical appeal of an enantioconvergent approach to the construction of quaternary stereocenters, only isolated examples have been reported to date.[9,13,14]

Over the past decade, chiral, dual hydrogen-bond-donor (HBD) catalysts have been developed that promote enantioselective nucleophilic substitution and addition reactions via ion pair intermediates. These catalysts promote ion pair formation via direct anion abstraction[15] or by substrate protonation with a co-catalytic Brønsted acid.[16] Asymmetric induction is typically achieved from the resultant ion pair as a consequence of specific attractive non-covalent interactions between the corresponding cationic intermediate and the chiral HBD catalyst.[17,18,19] Reported examples have been limited to heteroatom-stabilized cations, due to the challenges in *generating* the requisite ion pair and *suppressing* elimination/rearrangement pathways. The ability of HBD catalysts to control enantioselective nucleophile addition into non-heteroatom stabilized carbocations has to our knowledge not been demonstrated.

Recently, our group discovered that chiral squaramide catalysts could be used in conjunction with Lewis acids such as trimethylsilyl trifluoromethanesulfonate (TMSOTf) to promote enantioselective reactions.[20] This dual-catalyst system was shown to promote the formation of oxocarbenium ions from dialkyl acetals – substrates that are unreactive under previously developed HBD-promoted reaction manifolds – while still engaging in attractive non-covalent interactions to achieve enantioinduction. We envisioned that the strong ionizing ability of this dual catalyst system could provide access to carbocationic intermediates lacking heteroatom stabilization, thus allowing us to examine whether small molecule H-bond donors can be used to promote productive, enantioselective reaction pathways from such high energy intermediates.

Reaction development

After an extensive evaluation of potential tertiary electrophile–*C*-centered nucleophile coupling partners, the reaction of propargyl acetate **2a** with allyltrimethylsilane was identified as a useful model system to test this proposal (Figure 1c). In the absence of added HBD catalyst, the Lewis acid-promoted reaction affords a 1:1 mixture of desired product **3a** to elimination product **4a** (Figure 1c, entry 1). When readily accessed squaramide **1a** (10 mol %) was added to the reaction, however, **3a** was obtained in high yield (40:1, **3a:4a**; Figure 1c, entry 2) and enantioselectivity (91% e.e.). Product ratio and enantioselectivity

were strongly dependent on the nature of the HBD moiety: corresponding *N,N*-dimethylated squaramide (**1b**), thiourea (**1c**) and urea catalysts (**1d)** afforded **3a** in low yield and e.e. (Figure 1c, entry 3–5). No reaction was observed with squaramide, thiourea, or urea HBD catalysts in the absence of TMSOTf.

A series of tertiary propargyl acetates was subsequently evaluated in order to probe the reaction scope and to generate preliminary information about the mechanism of the enantioselective substitution reaction (Figure 2a). Substrates bearing electron-donating (e.g. **2b** and **2c**) and electron-withdrawing substituents (**2d**) underwent allylation in high enantioselectivity (>90% e.e.) and product selectivity (>30:1 **3:4**). A linear correlation with a small negative slope ($\rho^+ = -0.43$, Figure 2b) was observed between Hammett substituent σ^+ constants and log(e.r.) for substrates **2a**–**d**. In contrast, a linear correlation with a very large negative slope ($\rho^+ = -5.48$, Figure 2c) was obtained from the corresponding plot of σ^+ constants versus relative reaction rate ($\log(\nu_X/\nu_H)$) for the same substrates. The observation of a linear free-energy dependence (ρ^+) of this magnitude provides direct evidence of positive charge accumulation in the rate-determining transition state, consistent with an S_N1-type ionization mechanism.[21]

Despite the very subtle dependence of e.e. on the electronic properties of substrate substituents noted above, reaction enantioselectivity was strongly responsive to changes in the expanse and position of the aryl moiety of the substrate. A linear correlation was observed between polarizability values calculated for the aryl substituent,[22] and log(e.r.) of products **3a** and **3e**–**g** (Figure 2d), indicating that stabilizing aromatic interactions are likely to serve as a contributing factor in enantiodifferentiation.[23] Indeed, evidence for the existence of such stabilizing interactions could be gleaned from computational analysis of the putative complex between catalyst **1a** and substrate **2a** (Figure S9). Steric congestion near the reaction site also correlates with enantioselectivity. Thus, the *o*-tolyl-substituted derivative **2j** underwent the allylation reaction to afford product with higher e.e. (82%) than the *p*- and *m*-substituted analogs **2h** and **2i** (66–67% e.e.). Similarly, ethyl-substituted product **3k** was obtained in higher e.e. (94%) than methyl-substituted product **3b** (c.f. 91% e.e.).

Substrates containing electron-rich heterocycles also underwent highly enantioselective substitution. Representative *S*– and *O*–heterocyclic substrates underwent reaction with allyltrimethylsilane to afford quaternary products (**3l**–**n**) in high yield and e.e., and with no detectable elimination by products. Following derivatization, the absolute stereochemistry of product **3b** was determined by X-ray crystallography (Figure 2e).

Mechanistic studies

A mechanistic study of the reaction between a representative tertiary propargyl acetate substrate and allyltrimethylsilane promoted by squaramide **1a** and TMSOTf was undertaken to glean insight into the underlying catalytic mechanism. The disappearance of **2b** could be monitored over the entire course of the reaction using *in situ* infrared spectroscopy. Plots of the rate versus concentration data obtained from a “same excess” experiment revealed good graphical overlay (Figure 3a), demonstrating that no catalyst decomposition or product

inhibition occurs over the course of the reactions.[24] The linearity of these plots further indicates that the reaction obeys a first-order rate dependence overall. Good overlay was also observed in the plots of the data obtained from "different-excess" experiments, revealing a first order rate dependence on [**2b**] and no rate dependence on the concentration of allyltrimethylsilane. These kinetic findings are consistent with a stepwise reaction mechanism where substrate C-O cleavage is turnover-limiting and nucleophile addition occurs in a post-turnover-limiting step (Figure 3b). Kinetic studies further revealed a sub-first-order dependence of reaction rate on [TMSOTf], and a first-order dependence of reaction rate on [**1a**] with a non-zero y-intercept. The kinetic dependence on the concentrations of both **1a** and TMSOTf is consistent with pre-equilibrium formation of a resting state **1a**•TMSOTf complex that reacts directly with substrate **2**. The non-zero y-intercept is congruent with a competing background reaction observed in the absence of **1a** (see Supplementary Information). The observation that optimal enantioselectivities are obtained under conditions where a background, uncatalyzed reaction is expected is intriguing, and the subject of continued study.

With squaramide-TMSOTf-promoted formation of the carbocationic intermediate established as rate-limiting, a series of experiments was performed to interrogate the critical post rate-limiting steps. The formation of elimination byproduct was determined to be irreversible on the basis of a crossover experiment in which 1-naphthyl-substituted enyne **4a** (0.25 equiv) was introduced to the reaction of 2-naphthyl-substituted acetate, **2f**, under otherwise standard reaction conditions. This reaction afforded an 80% yield of 2-naphthyl-substituted product **3f**, and alkene **4a** was recovered in 97% yield with no trace of 1-naphthyl allylated product **3a** detected (Figure 4a).

To evaluate whether the reaction proceeds through an enantioselective or enantiospecific mechanism, the allylation was carried out by subjecting scalemic substrate (–)-**2f** (81% e.e.) to both enantiomers of the squaramide catalyst **1a** (Figure 4b). After 1h reaction time, product **3f** was obtained in 86% e.e. and 24% yield using (*S*)-**1a**; in the presence of (*R*)-**1a**, product **3f** was obtained in similar yield but with opposite enantioselectivity (−85% e.e.). In both cases, the recovered substrate **2f** was observed to have undergone only a small degree of epimerization, comparable to that observed when **2f** was treated with TMSOTf and in the absence of squaramide catalyst. The results of these experiments are consistent with a stereoablative mechanism, i.e. an enantioselective process that proceeds through an achiral carbocationic intermediate. In contrast, a dynamic kinetic resolution pathway can be ruled out where **2f** undergoes rapid racemization and one enantiomer preferentially undergoes stereospecific substitution.

Two limiting mechanistic possibilities were considered with regard to the enantiodetermining C–C bond-forming step: (a) irreversible nucleophile addition followed by rapid silyl elimination (Figure 4c, top), or (b) rapid and reversible nucleophile addition, followed by e.e.-determining silyl elimination (Figure 4c, bottom). These two scenarios are predicted to produce different carbon isotope effects at the allyl fragment. The carbon kinetic isotope effects (KIEs) were determined with natural abundance materials using Singleton's NMR methodology (Figure 4c, see supplementary materials).[25] A significant primary KIE of 1.027 was observed at the position of bond formation (internal allylic

methylene), while no KIE was observed at the terminal position. These results demonstrate that the first C–C bond-forming step is irreversible, therefore enantiodetermining.

Conclusion

The cooperative effect of chiral squaramides and TMSOTf was shown to generate tertiary carbocations lacking heteroatom stabilization from racemic precursors, control enantioselectivity in additions of a *C*-centered nucleophile, and attenuate undesired elimination pathways. The strategy outlined here may be generalizable to the construction of many types of highly congested stereogenic centers.

Supplementary Material

Refer to Web version on PubMed Central for supplementary material.

Acknowledgments

Financial support for this work was provided by the NIH through GM043214 and a postdoctoral fellowship to AEW. We thank Scott McCann and Dr. Charlie Fry for assistance with NMR experiments, Dr. Eugene E. Kwan for helpful discussions regarding the KIE studies, and Dr. Shao-Liang Zheng for X-ray determination.

References

1. Quasdorf KW, Overman LE. Catalytic enantioselective synthesis of quaternary carbon stereocentres. Nature. 2014; 516:181–191. [PubMed: 25503231]
2. Liu Y, Han SJ, Liu WB, Stoltz BM. Catalytic Enantioselective Construction of Quaternary Stereocenters: Assembly of Key Building Blocks for the Synthesis of Biologically Active Molecules. Acc Chem Res. 2015; 48:740–751. [PubMed: 25715056]
3. Das JP, Marek I. Enantioselective synthesis of all-carbon quaternary stereogenic centers in acyclic systems. Chem Commun. 2011; 47:4593–4623.
4. Feng J, Holmes M, Krische MJ. Acyclic Quaternary Carbon Stereocenters via Enantioselective Transition Metal Catalysis. Chem Rev. 2017; 117:12564–12580. [PubMed: 28910092]
5. Wilson RM, Jen WS, MacMillan DWC. Enantioselective Organocatalytic Intramolecular Diels −Alder Reactions. The Asymmetric Synthesis of Solanapyrone D. J Am Chem Soc. 2005; 127:11616–11617. [PubMed: 16104734]
6. Krautwald S, Sarlah D, Schafroth MA, Carreira EM. Enantio- and Diastereo-divergent Dual Catalysis: α-Allylation of Branched Aldehydes. Science. 2013; 340:1065. [PubMed: 23723229]
7. Behenna DC, Stoltz BM. The Enantioselective Tsuji Allylation. J Am Chem Soc. 2004; 126:15044–15045. [PubMed: 15547998]
8. Murphy JJ, Bastida D, Paria S, Fagnoni M, Melchiorre P. Asymmetric catalytic formation of quaternary carbons by iminium ion trapping of radicals. Nature. 2016; 532:218–222. [PubMed: 27075098]
9. Zhang P, Le H, Kyne RE, Morken JP. Enantioselective Construction of All-Carbon Quaternary Centers by Branch-Selective Pd-Catalyzed Allyl–Allyl Cross-Coupling. J Am Chem Soc. 2011; 133:9716–9719. [PubMed: 21648464]
10. Jung B, Hoveyda AH. Site- and Enantioselective Formation of Allene-Bearing Tertiary or Quaternary Carbon Stereogenic Centers through NHC–Cu-Catalyzed Allylic Substitution. J Am Chem Soc. 2012; 134:1490–1493. [PubMed: 22214185]
11. Mei TS, Patel HH, Sigman MS. Enantioselective construction of remote quaternary stereocentres. Nature. 2014; 508:340–344. [PubMed: 24717439]

12. Bhat V, Welin ER, Guo X, Stoltz BM. Advances in Stereoconvergent Catalysis from 2005 to 2015: Transition-Metal-Mediated Stereoablative Reactions, Dynamic Kinetic Resolutions, and Dynamic Kinetic Asymmetric Transformations. Chem Rev. 2017; 117:4528–4561. [PubMed: 28164696]
13. Braun M, Kotter W. Titanium(IV)-Catalyzed Dynamic Kinetic Asymmetric Transformation of Alcohols, Silyl Ethers, and Acetals under Carbon Allylation. Angew Chem Int Ed. 2004; 43:514–517.
14. Zhao W, Wang Z, Chu B, Sun J. Enantioselective Formation of All-Carbon Quaternary Stereocenters from Indoles and Tertiary Alcohols Bearing A Directing Group. Angew Chem Int Ed. 2015; 54:1910–1913.
15. Reisman SE, Doyle AG, Jacobsen EN. Enantioselective Thiourea-Catalyzed Additions to Oxocarbenium Ions. J Am Chem Soc. 2008; 130:7198–7199. [PubMed: 18479086]
16. Xu H, Zuend SJ, Woll MG, Tao Y, Jacobsen EN. Asymmetric Cooperative Catalysis of Strong Brønsted Acid–Promoted Reactions Using Chiral Ureas. Science. 2010; 327:986. [PubMed: 20167783]
17. Brak K, Jacobsen EN. Asymmetric Ion-Pairing Catalysis. Angew Chem Int Ed. 2013; 52:534–561.
18. Kennedy CR, Lin S, Jacobsen EN. The Cation–π Interaction in Small-Molecule Catalysis. Angew Chem Int Ed. 2016; 55:12596–12624.
19. Neel AJ, Hilton MJ, Sigman MS, Toste FD. Exploiting non-covalent π interactions for catalyst design. Nature. 2017; 543:637–646. [PubMed: 28358089]
20. Banik SM, Levina A, Hyde AM, Jacobsen EN. Lewis Acid Enhancement by Hydrogen-Bond Donors for Asymmetric Catalysis. Science. 2017; 358:761–764. [PubMed: 29123063]
21. Brown HC, Okamoto Y. Substituent Constants for Aromatic Substitution. J Am Chem Soc. 1957; 79:1913–1917.
22. McKinney JD, Gottschalk KE, Pedersen L. The polarizability of planar aromatic systems. An application to polychlorinated biphenyls (PCB's), dioxins and polyaromatic hydrocarbons. J Mol Struc-THEOCHEM. 1983; 105:427–438.
23. Hunter CA, Sanders JKM. The nature of. pi.-.pi interactions. J Am Chem Soc. 1990; 112:5525–5534.
24. Blackmond DG. Reaction Progress Kinetic Analysis: A Powerful Methodology for Mechanistic Studies of Complex Catalytic Reactions. Angew Chem Int Ed. 2005; 44:4302–4320.
25. Singleton DA, Thomas AA. High-Precision Simultaneous Determination of Multiple Small Kinetic Isotope Effects at Natural Abundance. J Am Chem Soc. 1995; 117:9357–9358.

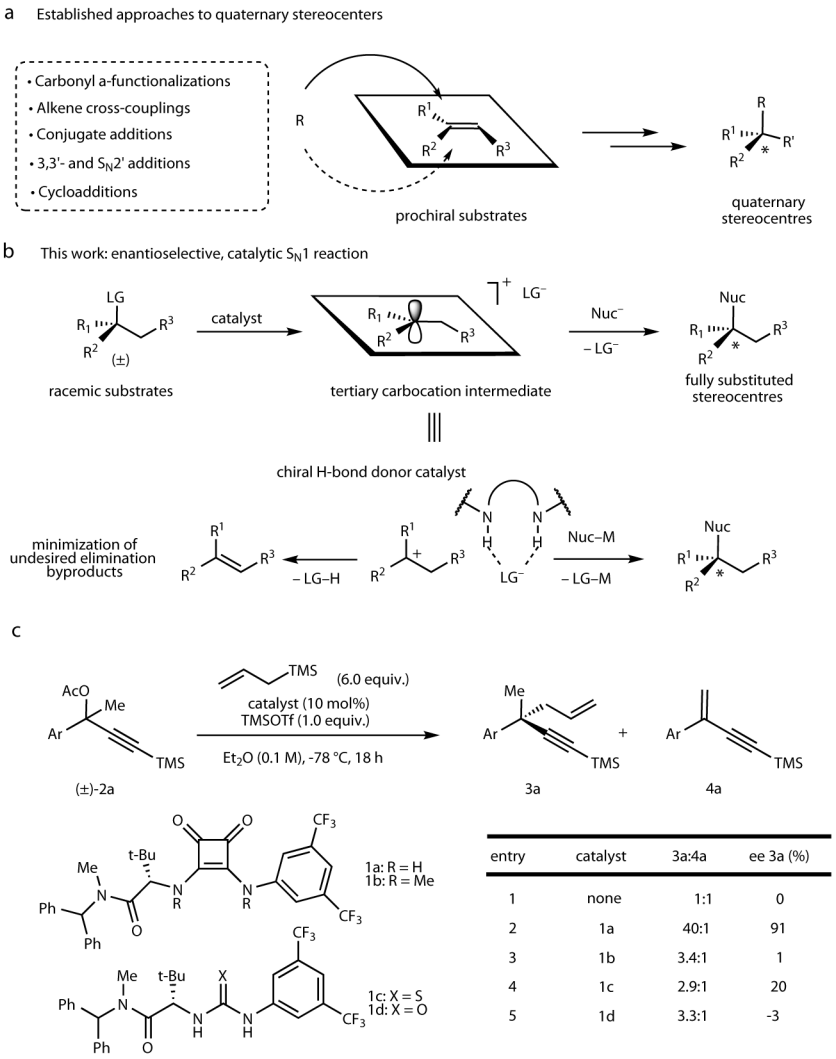

entry	catalyst	3a:4a	ee 3a (%)
1	none	1:1	0
2	1a	40:1	91
3	1b	3.4:1	1
4	1c	2.9:1	20
5	1d	3.3:1	-3

Figure 1. Approaches to the enantiocontrolled construction of quaternary stereocenters

a, Traditional methods for synthesis of quaternary stereocenter-containing molecules employ stereochemically defined prochiral substrates. **b**, S_N1 approach to the construction of quaternary stereocenters. **c**, Enantioselective allylation of propargyl acetates using chiral squaramide catalysts and TMSOTf promoter. TMS, trimethylsilyl; Np, naphthyl.

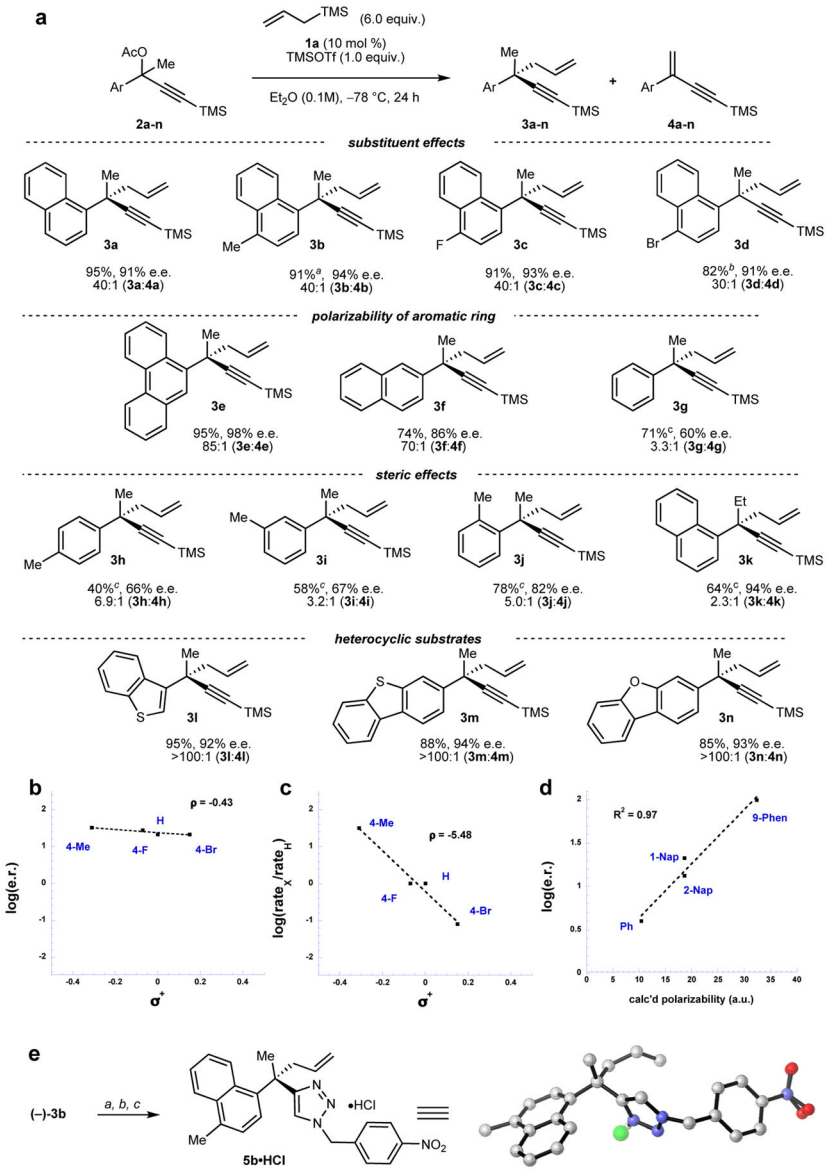

Figure 2. Asymmetric allylation of propargyl acetates

a, Substrate scope. Reactions were run on 0.6 mmol scale with 0.1 equiv. **1a**, 1.0 equiv. TMSOTf, and 6.0 equiv. allyltrimethylsilane in 0.1M Et_2O at −78 °C for 24 h. [a] Reaction time was 4 h. [b] Reaction time was 14 d. [c] NMR yield. **b,** Hammett plot of σ^+ values of substituents in **2a**–**d** versus enantiomer ratios obtained in the formation of **3a**–**d. c,** Hammett plot of σ^+ values on substituents in **2a**–**d** versus relative reaction rates determined for each substrate. **d,** Linear free energy plot of the calculated polarizability of the aromatic rings in **2a**, **2e**–**g** versus enantiomer ratios obtained in the formation of **3a, 3e**–**g. e,** The absolute configuration of (–)-**3b** was determined by X-ray crystallography (structure shown), following derivatization to triazole **5b**; the configuration of all other products was assigned by analogy. Conditions: (*a*) TBAF (2.0 equiv.), THF, r.t.; (*b*) 4-nitrobenzylbromide (1.1

equiv.), NaN_3 (1.1 equiv.), $CuSO_4$ (0.1 equiv.), sodium ascorbate (0.2 equiv.), *t*BuOH/H_2O (1:2), 50 °C; (*c*) HCl (3M in Et_2O).

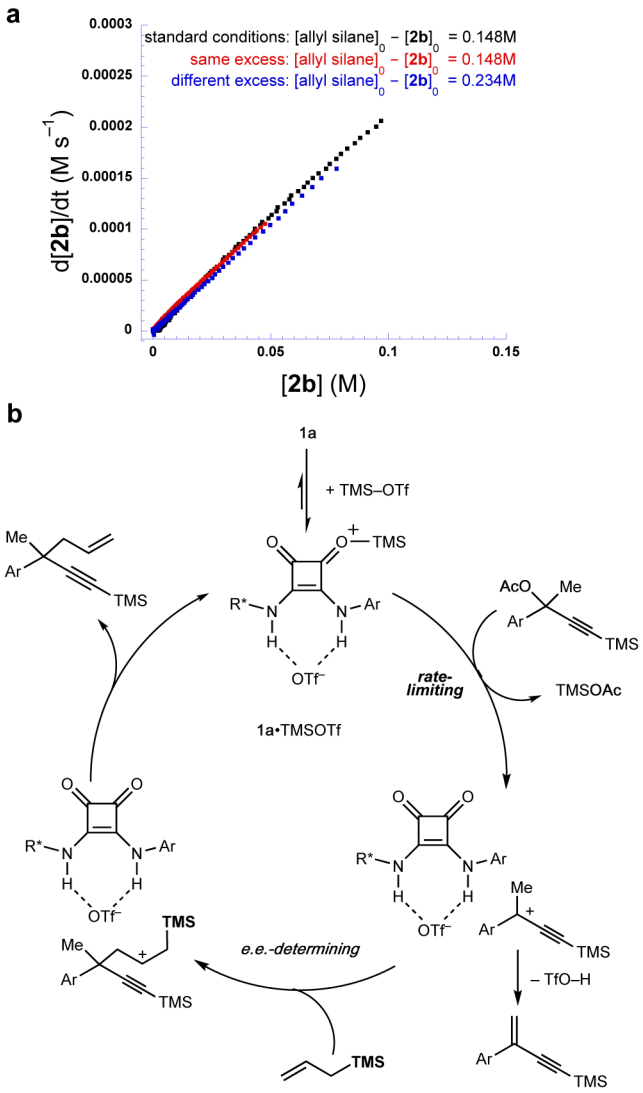

Figure 3. Kinetic data and catalytic cycle

a, Reaction progress kinetic analysis of the reaction of **2b** with allyltrimethylsilane. 0.047M; [allyltrimethylsilane]$_0$ = 0.195M; different excess: [**2b**]$_0$= 0.08M; [allyltrimethylsilane]$_0$ = 0.315M. **b**, Proposed catalytic mechanism for the enantioselective allylation of propargyl acetates.

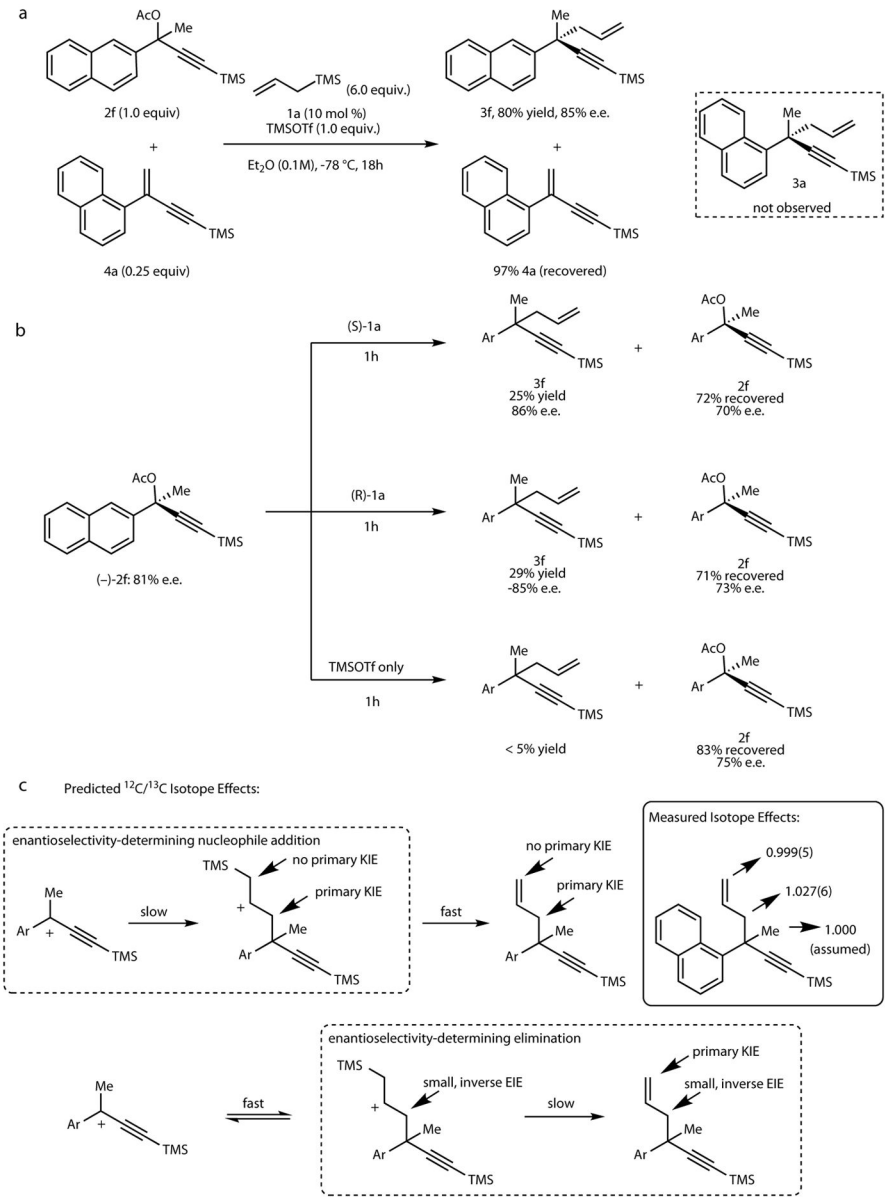

Figure 4. Mechanistic studies probing the post-rate-limiting steps of the allylation reaction

a, Crossover experiment establishing irreversible formation of alkene byproduct. **b**, Partial reaction with scalemic **2g** demonstrating that allylation proceeds via a stereoablative mechanism rather than by a dynamic kinetic resolution process. **c**, Predicted and measured $^{12}C/^{13}C$ kinetic isotope effects (KIEs).